International Journal of Solids and Structures 54 (2015) 172–182

Contents lists available at ScienceDirect

International Journal of Solids and Structures

journal homepage: www.elsevier.com/locate/ijsolstr

High strain rate behaviour of 5-harness-satin weave fabric carbon–epoxy composite under compression and combined compression–shear loading

H. Koerber [a,*], J. Xavier [b], P.P. Camanho [c], Y.E. Essa [d], F. Martín de la Escalera [d]

[a] Institute for Carbon Composites, Technische Universität München, Faculty of Mechanical Engineering, Boltzmannstrasse 15, 85748 Garching bei München, Germany
[b] Optics and Experimental Mechanics Laboratory, INEGI, Campus da FEUP, Rua Dr. Roberto Frias, 4200-465 Porto, Portugal
[c] DEMec, Faculdade de Engenharia, Universidade do Porto, Rua Dr. Roberto Frias, 4200-465 Porto, Portugal
[d] Aernnova Engineering Solutions Ibérica S.A., Avenida de Manoteras 20, 28050 Madrid, Spain

ARTICLE INFO

Article history:
Received 16 January 2014
Received in revised form 8 September 2014
Available online 28 October 2014

Keywords:
Polymer–matrix composites
Strain-rate effects
Plastic deformation
Failure envelopes
Digital image correlation

ABSTRACT

The strain rate dependent mechanical behaviour was studied for the common out-of-autoclave aerospace textile composite 5-harness-satin carbon–epoxy. End-loaded 15°, 30° and 45° off-axis and 90° compression tests were carried out at three different strain rate levels ($4 \times 10^{-4}\ \mathrm{s}^{-1}, 200\ \mathrm{s}^{-1}$ and $1000\ \mathrm{s}^{-1}$) to determine the effect of strain rate for transverse compression and combined transverse compression/in-plane shear loading. The dynamic tests were carried out on a split-Hopkinson pressure bar, where high speed photography and digital image correlation allowed a detailed study of the specimen deformation and failure process. Quasi-static reference tests were carried out on an electro-mechanical test machine using the same specimen type and a static DIC system. Pronounced strain rate effects on the axial stress–strain response were observed for all specimen types. Failure envelopes for the combined $\sigma_{22}^{c} - \tau_{12}$ stress state were derived from the experimental data and compared with the maximum stress criterion, which appears well suited to approximate the experimental failure envelope at all strain rate levels. It was observed that the failure envelope was simply scaled up with increasing strain rate, while the overall shape was found to be strain rate independent.

1. Introduction

The strain rate dependency of fibre reinforced polymer matrix composites (FRPMCs) is well known and has received significant attention from the scientific community over the past decades. Comprehensive review articles on this matter were presented by Sierakowski (1997) and Jacob et al. (2004). An overview of typical experimental techniques for high strain rate testing of FRPMCs was given by Hamouda and Hashmi (1998) and for general materials by Gray (2000). A good review of the split-Hopkinson pressure bar method, used for the dynamic tests in this paper, was presented by Gama et al. (2004).

The interest in the study of high strain rate behaviour continues with increasing applications of FRPMCs in primary structures of modern aircraft and future composite intensive cars, all which are subjected to high strain rate loading conditions. Recent studies on the high strain rate behaviour of polymer composites were based on UD glass–epoxy (Tsai and Sun, 2005; Shokrieh and Omidi, 2009, 2011; Gerlach et al., 2013), UD carbon–epoxy (Hsiao and Daniel, 1998; Hsiao et al., 1999; Hosur et al., 2001; Gilat et al., 2002; Bing and Sun, 2005; Taniguchi et al., 2007; Koerber et al., 2010; Koerber and Camanho, 2011; Daniel et al., 2011; Schaefer et al., 2014), 2D and 3D woven (Hosur et al., 2004; Guden et al., 2004; Naik and Venkateswara, 2008; Ravikumar et al., 2013; Chen et al., 2013; Pankow et al., 2011; Gerlach et al., 2012) and braided composites (Salvi et al., 2009).

The majority of the studies, which have used split-Hopkinson bars for the dynamic tests, have either determined the axial stress–strain response of the specimen by using classical split-Hopkinson pressure bar analysis (SHPBA), where both the specimen stress-time and the specimen strain–time response are calculated from the strain waves measured on the bars, or have measured the specimen strain directly on the specimen, using foil strain gauges.

Due to readily available high speed camera technology with sufficient resolution to apply optical and therefore contactless strain field measurement techniques such as digital image correlation

---

* Corresponding author. Tel.: +49 (0)89 289 15042; fax: +49 (0)89 289 15097.
E-mail address: koerber@lcc.mw.tum.de (H. Koerber).

http://dx.doi.org/10.1016/j.ijsolstr.2014.10.018
0020-7683/© 2014 Elsevier Ltd. All rights reserved.

(DIC) (Sutton et al., 2009; Pan et al., 2009), unique data reduction possibilities are now offered for high strain rate material characterisation.

2D or 3D specimen displacement and strain fields can be obtained (depending on the availability of a stereo-vision setup, utilising two instead of one high speed camera). The specimen strain can be obtained over a large strain range, exceeding the typical range of foil strain gauges. The specimen deformation and failure mechanisms can be studied as they occur and the uniformity of the specimen strain field can be evaluated. Those advantages and possibilities have recently been demonstrated for the dynamic material characterisation of UD glass fibre (Gerlach et al., 2013), UD carbon fibre (Koerber et al., 2010), 3D-woven glass fibre (Pankow et al., 2011), 3D-woven carbon fibre (Gerlach et al., 2012) composites and for ductile metals (Gilat et al., 2009).

Despite many earlier studies on the high strain rate mechanical response of FRPMCs, which have contributed significantly to the understanding of the dynamic material behaviour of composites, further studies are justified by the significant improvements now offered by high speed photography and optical strain measurement techniques. The thus determined specimen stress–strain behaviour as well as a clear identification of damage initiation and failure mechanisms are needed to improve and further develop composite material models, able to predict experimentally observed strain rate dependent nonlinearities under multi-axial loading conditions prior to the onset of cracking as well as progressive evolution of damage until ultimate failure (Vogler et al., 2013a,b).

The objective of this work is to study the strain rate effect on the in-plane mechanical behaviour of the common aerospace textile composite 5-harness-satin carbon–epoxy. The material was subjected to combined compression/in-plane shear loading using off-axis compression specimens at three different strain rate levels ($4 \times 10^{-4}\ \mathrm{s}^{-1}, 200\ \mathrm{s}^{-1}$ and $1000\ \mathrm{s}^{-1}$). Static and high strain rate tests were performed, using DIC to obtain the true stress–strain response and identify damage initiation and evolution at all strain rate levels. Failure envelopes were derived from the experimental data and compared with a suitable failure criterion. The herein presented static and dynamic specimen strain field data may be used for the validation of finite element simulations using advanced composite material models. To the knowledge of the authors, no such data yet exists for the composite material system and strain rates investigated in this study.

2. Material and specimen type

The investigated material system 5-harness-satin carbon–epoxy represents a balanced 2D woven textile composite (equal amount of fibres in warp and weft direction). A plate was manufactured via the resin transfer moulding (RTM) process, using a standard aerospace qualified epoxy resin system for RTM processes. To obtain a nominal panel thicknesses of 4 mm at a given cured ply thickness of 0.363 mm, a layup of $[0]_{11}$ was chosen.

From this panel rectangular end-loaded type $15^\circ, 30^\circ$ and 45° off-axis compression and 90° (weft direction) compression specimens were cut using a water-cooled diamond saw. Polishing of the loading surfaces ensured a parallelism of ≤ 0.02 mm. The nominal specimen dimensions were $20 \times 10 \times 4\ \mathrm{mm}^3$ (*length* × *width* × *thickness*) for the quasi-static and intermediate and $10 \times 10 \times 4\ \mathrm{mm}^3$ for the high strain rate tests. A reduction of the specimen length and an increase of the striker bar velocity was chosen to obtain significantly higher strain rates for the second rate regime on the SHPB without pushing the velocity of the striker bar and the subsequent inertia forces on the bar strain gauges beyond the limit of the SHPB apparatus used in this study.

The planar rectangular specimen geometry had proven to be very effective in an earlier study (Koerber et al., 2010) and was therefore adopted for the present work. A detailed study on wether specimen geometry (different length-to-diameter L/D ratios for cylindrical specimens and the comparison of cylindrical with square/rectangular shapes) has an effect on the results of high strain rate compression tests for UD composite materials, was performed by Woldesenbet and Vinson (1999). It was concluded that no statistically significant effects could be found for either L/D ratio or specimen shape. It was further concluded that it is eligible to use different specimen lengths to obtain different strain rates on the Hopkinson bar apparatus, as done in this study.

To prepare the specimens for DIC measurement, a random black-on-white speckle pattern was applied using aerosol spray painting. Three tests were performed for each specimen type and strain rate regime.

3. Experimental setup

3.1. Quasi-static experimental setup

The quasi-static reference tests were carried out on an electromechanical universal test machine of the type INSTRON 4208 at a constant displacement rate of $0.5\ \mathrm{mm\,min}^{-1}$. Considering the nominal specimen length of 20 mm, all specimens were loaded at an axial strain rate of $\dot{\varepsilon}_{qs} \approx 4 \times 10^{-4}\ \mathrm{s}^{-1}$. The static self-aligning end-loaded compression setup is shown in Fig. 1. Polished tungsten-carbide (TC) inserts were used to avoid damage of the loading faces of the test fixture due to the high compressive strength of the specimen in fibre direction. Friction between the TC-inserts and the specimen was minimised by a thin layer of Molybdenum-Disulfide (MoS_2).

The GOM ARAMIS® system was used to obtain the quasi-static specimen strain field. It consisted of an 8-bit Baumer Optronic FWX20 camera with a resolution of $1624 \times 1236\ \mathrm{pixel}^2$, coupled with a Nikon AF Micro-Nikkor 200 mm f/4D IF-ED lens and a 50 mm extension tube. The camera was positioned at a distance of 1 m away from the specimen surface. Two Raylux 25 white-light LEDs on either side of the camera guaranteed an even illumination of the specimen surface. The acquisition rate of the camera was set to 1 frame per second (fps) with a shutter speed of 40 ms and an aperture of $f/11$. The analysis parameters chosen for the quasi-static DIC measurements are given in Table 1. In this configuration, the resolution in displacement and strain are typically about 10^{-2} pixels and 0.02%, respectively (Xavier et al., 2012).

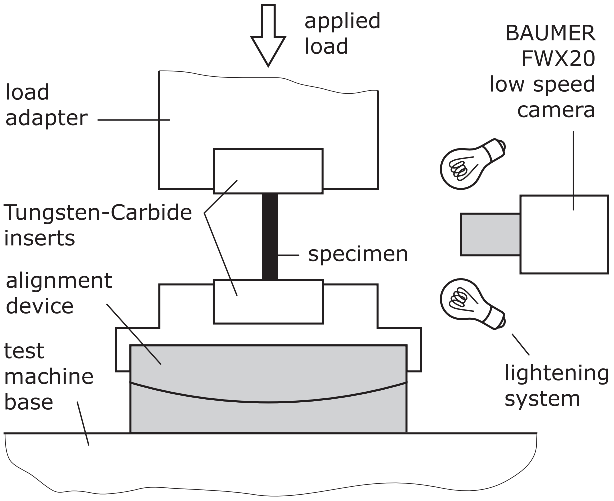

Fig. 1. Quasi-static compression test setup.